Contour Matching for 3D Ear Recognition

Hui Chen and Bir Bhanu
Center for Research in Intelligent Systems
University of California, Riverside, California 92521, USA
{bhanu,hchen}@vislab.ucr.edu

Abstract

Ear is a new class of relatively stable biometric that is invariant from childhood to early old age (8 to 70). It is not affected with facial expressions, cosmetics and eye glasses. In this paper, we introduce a two-step ICP (Iterative Closest Point) algorithm for matching 3D ears. In the first step, the helix of the ear in 3D images is detected. The ICP algorithm is run to find the initial rigid transformation to align a model ear helix with the test ear helix. In the second step, the initial transformation is applied to selected locations of model ears and the ICP algorithm iteratively refines the transformation to bring model ears and test ear into best alignment. The root mean square (RMS) registration error is used as the matching error criterion. The model ear with the minimum RMS error is declared as the recognized ear. Experimental results on a dataset of 30 subjects with 3D ear images are presented to demonstrate the effectiveness of the approach.

1. Introduction

Ear is a viable new class of biometrics since the ear has desirable properties such as universality, uniqueness and permanence [9, 10]. Although it has certain advantages over other biometrics, it has received little attention compared to other popular biometrics such as face, fingerprint and gait. For example, ear is rich in features; it is a stable structure which does not change with the age; it doesn't change its shape with facial expressions, cosmetics and hair styles.

In recent years, some approaches have been developed for the ear recognition from 2D images. Burge and Burger [4] proposed an adjacency graph, which is built from the Voronoi diagram of the ear's edge segments, to describe the ear. Ear recognition is done by subgraph matching. Hurley et al. [8] applied force field transform to ear images and wells and channels are shown to be invariant to affine transformations. Chang et al. [6] used principal component analysis to ear images. All of these work for ear recognition have used 2D intensity images and therefore the performance of their systems is greatly affected by imaging conditions such as lighting and shadow. However currently avail-

able range sensors can directly provide us 3D geometric information which is insensitive to above imaging problems. Therefore, it is desirable to design a human ear recognition system from 3D side face images obtained at a distance. In fact, different methods to design biometrics system based on 3D data have been addressed [2, 3, 5, 7, 11, 12, 14].

In this paper, we describe a two-step ICP (Iterative Closest Point) procedure for matching 3D ears. ICP algorithm is to match a data shape Y to a model shape X by iteratively minimizing the distance between corresponding pairs. In the training phase, the helixes of model ears in 3D images are extracted and saved. In the testing phase, the helix of the test ear in 3D image is detected. For each model ear helix, we run the ICP algorithm to find the initial rigid transformation which aligns a model ear helix with the test ear helix. After this, we have a set of rigid transformations for each model-test pair. Then by applying the initial rigid transformation obtained previously to selected control points of the model ear, we run ICP to improve the transformation which brings model ear and test ear into best alignment, for every model-test pair. The root mean square (RMS) registration error is used as the matching error criterion. The model ear with the minimum RMS error is declared as the recognized ear.

The rest of the paper is organized as follows. Section 2 describes our approach to automatic detection of ear helixes and matching ears. Section 3 provides the experimental results to demonstrate the effectiveness of our approach. Finally, Section 4 presents conclusions.

2. Technical approach

The system block diagram is illustrated in Fig. 1. Our approach has three main steps: 1) automatic ear helix detection; 2) first-step ICP to align the model ear helix with the test ear helix and to obtain the initial rigid transformation; 3) second-step ICP to refine the transformation.

2.1 Ear helix detection

To detect ear helix in intensity images is not a trivial task. However in range images there are strong depth discontinuities around the ear helix. The step edge magnitude, de-
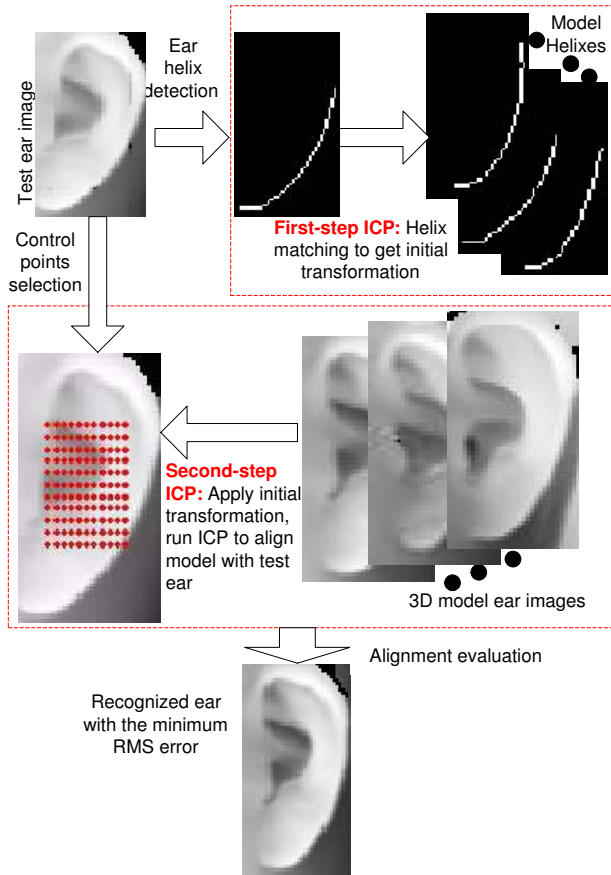
Figure 1. System diagram.

noted by L_{step}, is calculated as the maximum distance in depth between the center point and its neighbors in a small window [15]. L_{step} can be formulated as follows:

$$L_{step}(i,j) = max|z(i,j) - z(i+k,j+l)| \quad (1)$$
$$-(w-1)/2 \le k, l \le (w-1)/2$$

where w is the width of the window and $z(i,j)$ is the z coordinate of the point(i,j). To get the step edge magnitude image, a $w \times w$ window is translated over the original ear range image and the maximum distance calculated from (1) replaces the pixel value of the pixel covered by the center of the window. The step edge magnitude is thresholded to get a binary edge image which is shown in Fig. 2(b), while the original ear range image is shown in Fig. 2(a). It's inevitable that we also get the unwanted edge segments, for instance, around the ear antihelix. We proceed to do edge thinning and linking and remove small edge segments; the result image is shown in Fig. 2(c). Furthermore, since we take the left ear range image and know the ear helix lies in the right side of image, we can remove edge segments which do not belong to the helix and the final detected helix of ear is shown in Fig. 2(d). The extracted ear helix is represented by a set of 3D coordinates $M = \{(x(i), y(i), z(i))\}, i = 1, 2, \ldots, p_m$ where p_m is the number of points on the detected ear helix. We repeat the same procedure for each model ear and get a set of 3D seg-

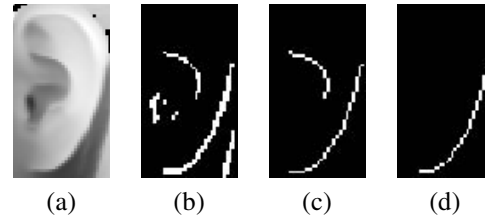ments $\{M_j, j = 1, 2, \ldots, N_m\}$ where N_m is the number of model ears.

(a)   (b)   (c)   (d)

Figure 2. Steps to automatically extract the helix of ear.

2.2 First-Step ICP

We can detect test ear helix using the same previous step. The detected test ear helix is represented by a set of 3D coordinates $S = \{(x(i), y(i), z(i))\}, i = 1, 2, \ldots, p_t$ where p_t is the number of points on the detected test ear helix. Given two sets of 3D points M_j and S, we like to find a rigid transformation T_r to align them such that the mean square error $E = \sum_{l=1}^{n} |T_r(M_{jl}) - S_l|^2$ is minimized. ICP algorithm developed by Besl and Mckay [1] is well-known method to align 3D shapes. However ICP requires that every point in one set have a corresponding point on the other set, we can't guarantee that detected ear helix satisfy this requirement. Therefore, we use a modified ICP algorithm presented by Turk [13] to register two helixes. We call this step ICP first-step ICP. The steps of modified ICP algorithm to register a test shape Y to a model shape X are:

1) Initialize the rotation matrix R_0 and translation vector T_0.

2) Given each point in Y, find the closest point in X.

3) Discard pairs of points which are too far apart.

4) Find the rigid transformation (R, T) such that E is minimized.

5) Apply the transformation (R, T) to Y.

6) Goto step 2) until the difference $|E_k - E_{k-1}|$ in two successive steps falls below a threshold ϵ or the maximum number of iterations is reached.

By initializing the rotation matrix R_0 and translation vector T_0 to the identity matrix and zero vector respectively, we run ICP iteratively and finally get the rotation matrix R_1 and translation vector T_1, which brings the model ear helix and test ear helix into alignment. R_1 and T_1 will be used as the initial transformation for the second-step ICP. The alignment is shown in Fig. 3. The detected model ear helix is marked by red pluses; the detected test ear helix is marked by black points; the model ear helix after registration is marked by blue circles. From Fig. 3, we can clearly see that the model ear helix is brought closer to the test ear helix. We apply the transformation R_1 and T_1 to the model ears and examples of model ears coarsely aligned to test ears are shown in Fig. 4 for model-test pairs 5, 10, 18 and 19. Furthermore, if we use the RMS errors from first-step ICP as matching error criterion, we would make 18 errors

out of 30. Therefore, it's necessary to do second-step ICP to improve the transformation, which can be justified by comparing the RMS errors for the same model-test pair in Fig. 4 and Fig. 9.

In summary, the purpose of the first-step ICP is: i) to align the model ear helix with the test ear helix which brings the model and test ear into coarse alignment; ii) to provide the initial rigid transformation for second-step ICP.
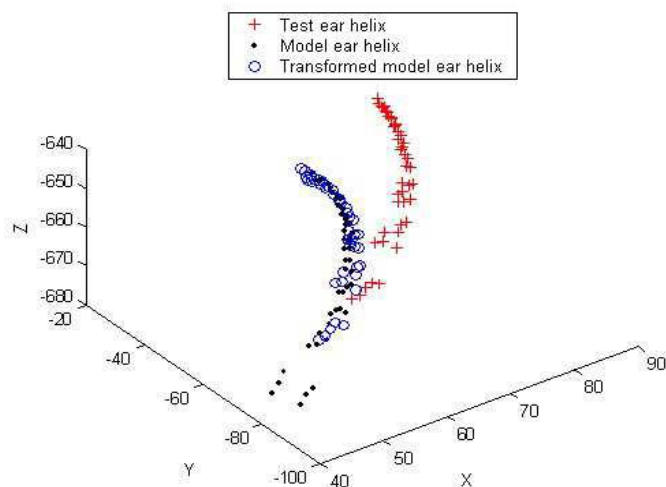

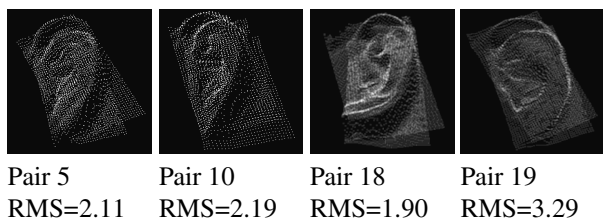**Figure 3. Alignment of model ear and test ear helixes.**

Pair 5	Pair 10	Pair 18	Pair 19
RMS=2.11	RMS=2.19	RMS=1.90	RMS=3.29

Figure 4. Examples of coarsely aligned model-test pairs in first-step ICP.

2.3 Second-Step ICP

Given the coarse match between model and test ear, the purpose of the second-step ICP is to determine if the match is good and to find a refined alignment between them. If the test ear is really an instance of the model ear, the second-step ICP algorithm will result in a good registration and more corresponding points between model and test ear surfaces will be found.

One way to evaluate the registration is to measure some distance between model and test; a good match will have a small distance. The simple way to measure the distance is to calculate the average distance between control points

in the model ear and the corresponding closest points in the test ear. Since the ear is assumed to be in the center of the image, the control points are selected around the center of the image.

In summary, the second-step ICP algorithm starts with the initial transformation R_1 and T_1 obtained from the first-step ICP, and iteratively refines the transformation by minimizing the distance between the control points of the model ear and their closest points of the test ear.

2.4 Recognition

We have two results from the second-step ICP: i) a rigid transformation which aligns the model and test ear; ii) a root mean square (RMS) registration error. The RMS error is used as the matching criterion. The model ear with the minimum RMS error is declared as the recognized ear.

3. Experimental results

3.1 Data acquisition

We use real range data acquired using Minolta Vivid Camera. The range image contains 200×200 grid points and each grid point has a 3D coordinate (x, y, z). There are 30 subjects in our database and every subject has two left side face range images taken at different viewpoints. The ears were manually extracted from side face images. The data is split into model and test sets. Each set has 30 ears. The average number of 3D points in the ears is 1947. The manually extracted model ears are shown in Figure 5.

Figure 5. Model ear images for ears 1-30 labeled from left to right and top to bottom.
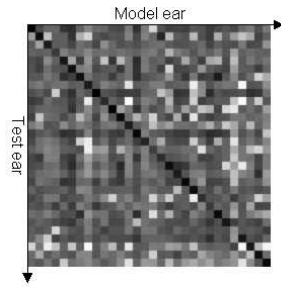
Figure 6. Matching error matrix displayed as an intensity image (smaller values corresponding to darker pixels).
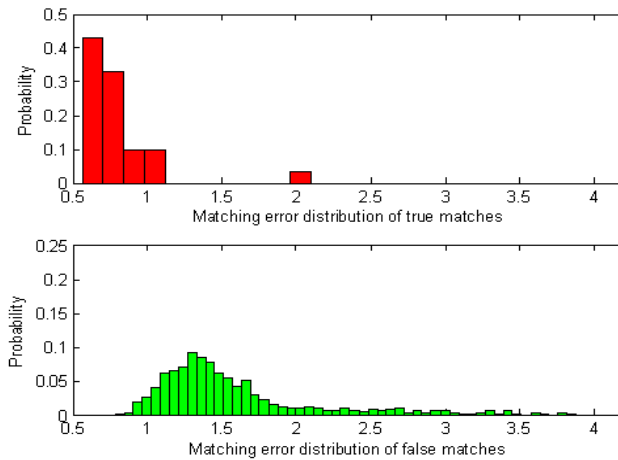

Figure 7. Matching error distributions for true-match and false-match.

3.2 Results

For every test ear, we run the two-step ICP procedure to match it with every model ear. The RMS registration errors are saved into the matching error matrix $\{ME(i,j), i = 1, 2, \ldots, N_t, j = 1, 2, \ldots, N_m\}$ where N_t and N_m are the number of test ears and model ears respectively. The matching error matrix is displayed as an intensity image shown in Fig. 6. The smaller the matching error is; the more likely the two ears are. From Fig. 6, we can see most of the diagonal pixels are darker than the other pixels on the same row, which means correct recognition. In our experiments, we achieved 93.3% recognition rate (2 errors out of 30). The matching error distribution for true matches and false matches is illustrated in Fig. 7. The minimum, maximum, mean and standard deviation for true-match and false-match are [0.56 1.96 0.79 0.26] and [0.78 3.81 1.57 0.53] respectively. In our experiment, there is an overlap between two distributions, which accounts for false matches.

The receiver operating characteristic (ROC) curve is defined as the plot of genuine acceptance rate against false acceptance rate. Fig. 8 shows the ROC curve of the proposed
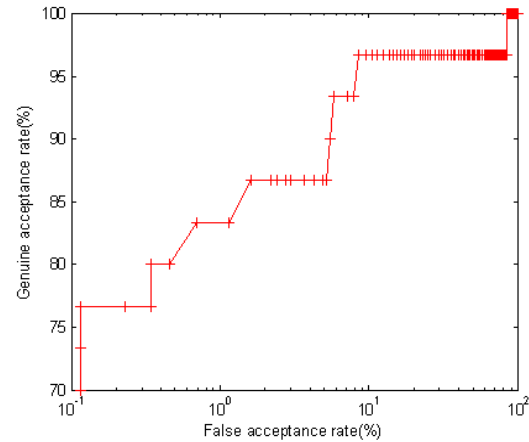

Figure 8. ROC curve of the experimental results.

approach on our database. The EER (equal-error rate) is 6.7%.

We show the correctly recognized model-test ear pairs and the RMS registration errors in Fig. 9. In order to evaluate our results, we display the model ear and test ear in the same image, the transformed model and test ear in the same image. With our programs, we can view them at different viewpoints. In Fig. 9, we only display them at a certain viewpoint. The images in the left four columns display test ears and their corresponding model ears before registration; the images in the right four columns show test ears and correctly recognized model ears after registration. From Fig. 9, we clearly see that the model ear is well aligned with the corresponding test ear.

During the recognition, we made two errors: ear 23 is falsely recognized as ear 9 and ear 26 is incorrectly recognized ear 30. The two error cases are illustrated in Fig. 10 by showing the model-test pairs before and after registration and the transformation parameters.

4. Conclusions

We have presented a two-step ICP procedure for the recognition of 3D ears. First-step ICP brings the model and test ear into coarse alignment; second-step ICP refines the transformation to nicely align the model ear with the test ear. Experimental results with 3D ear images show the effectiveness and potential of our approach for robust ear recognition in 3D. Despite these encouraging results, there is one issue to point out. Although RMS registration error used as the matching error criterion works for most of the cases, the registration produces a low RMS error in some cases. Incorporating other features into the verification step will be helpful.
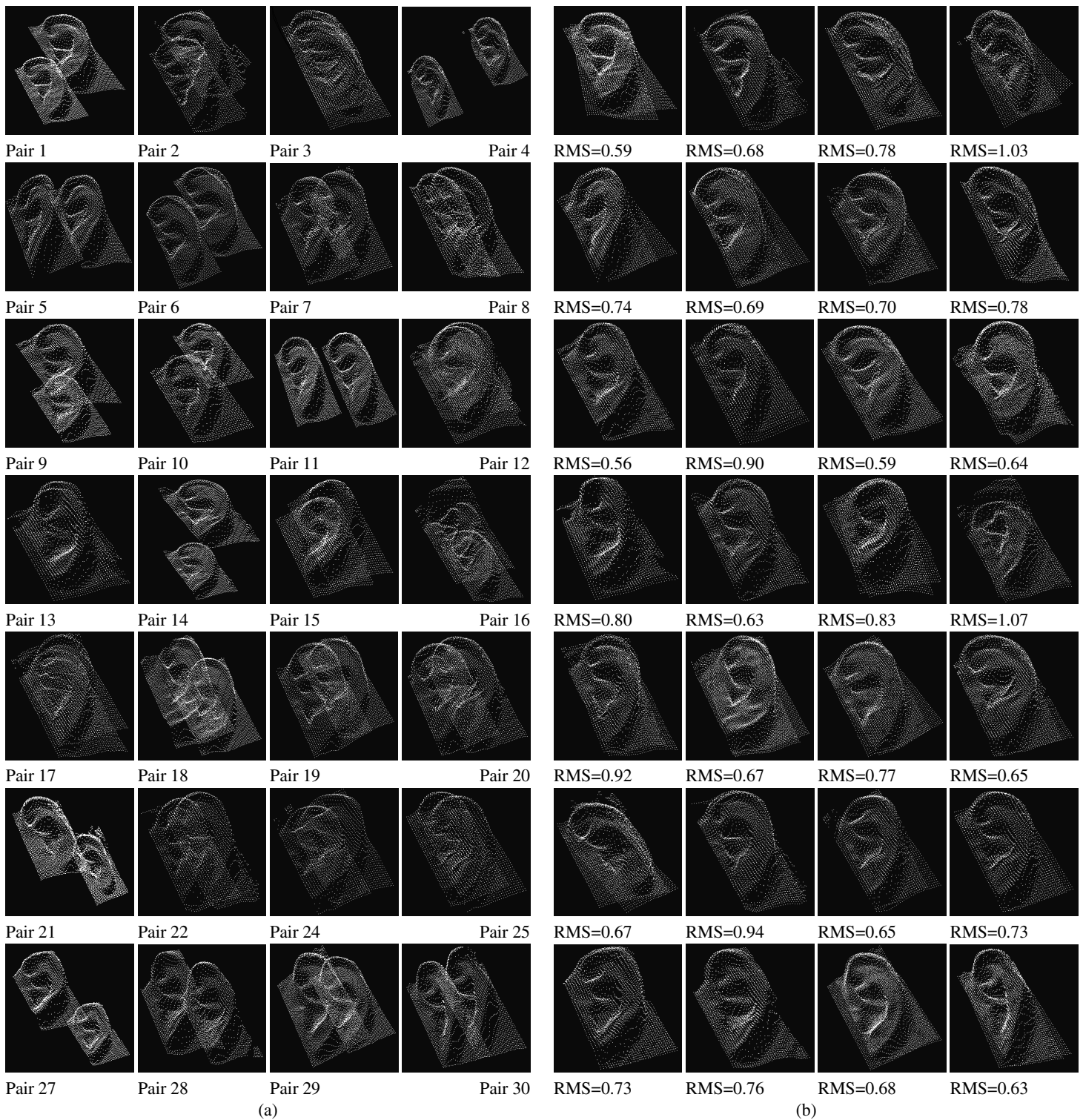
Pair 1	Pair 2	Pair 3	Pair 4	RMS=0.59	RMS=0.68	RMS=0.78	RMS=1.03
Pair 5	Pair 6	Pair 7	Pair 8	RMS=0.74	RMS=0.69	RMS=0.70	RMS=0.78
Pair 9	Pair 10	Pair 11	Pair 12	RMS=0.56	RMS=0.90	RMS=0.59	RMS=0.64
Pair 13	Pair 14	Pair 15	Pair 16	RMS=0.80	RMS=0.63	RMS=0.83	RMS=1.07
Pair 17	Pair 18	Pair 19	Pair 20	RMS=0.92	RMS=0.67	RMS=0.77	RMS=0.65
Pair 21	Pair 22	Pair 24	Pair 25	RMS=0.67	RMS=0.94	RMS=0.65	RMS=0.73
Pair 27	Pair 28	Pair 29	Pair 30	RMS=0.73	RMS=0.76	RMS=0.68	RMS=0.63

(a)   (b)

Figure 9. (a) 28 test ears with the corresponding model ears before registration. (b) 28 test ears with the correctly recognized model ears after registration.
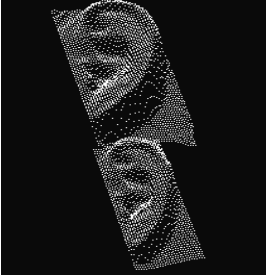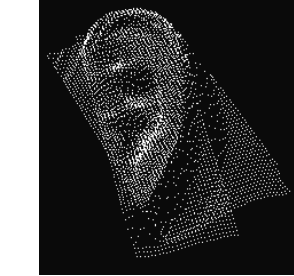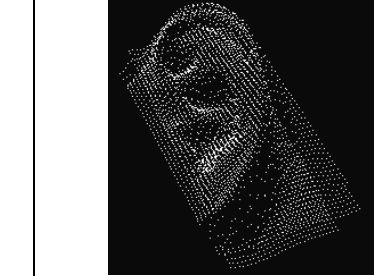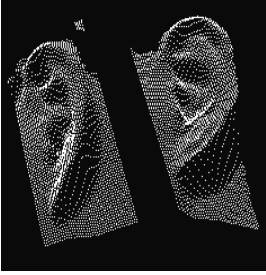
IEEE
COMPUTER
SOCIETY
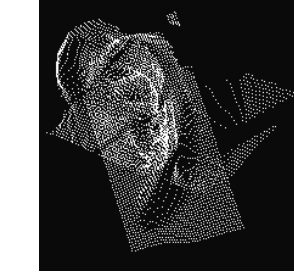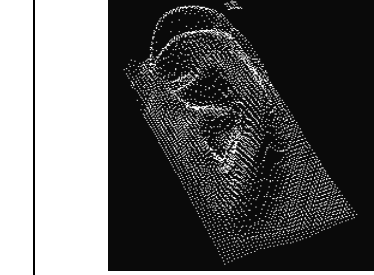
(a) Pair 23	(b) Pair 23 after registration	(c) Test ear 23 is falsely recognized as ear 9
The upper is model ear	$R=\begin{bmatrix} 0.9418 & -0.2224 & -0.2521 \\ 0.2475 & 0.9662 & 0.0723 \\ 0.2274 & -0.1305 & 0.9650 \end{bmatrix}$ $T=[-136.48\ 6.91\ -85.36]$ RMS=1.04	$R=\begin{bmatrix} 0.9935 & -0.0184 & -0.1119 \\ 0.0178 & 0.9998 & -0.0070 \\ 0.1120 & 0.0050 & 0.9937 \end{bmatrix}$ $T=[-128.25\ 3.36\ 32.43]$ RMS=1.03
(a) Pair 26	(b) Pair 26 after registration	(c) Test ear 26 is falsely recognized as ear 30
The right is model ear	$R=\begin{bmatrix} 0.5412 & -0.6122 & -0.5765 \\ 0.5917 & 0.7643 & -0.2563 \\ 0.5975 & -0.2024 & 0.7759 \end{bmatrix}$ $T=[-339.73\ -164.29\ -153.50]$ RMS=1.96	$R=\begin{bmatrix} 0.9978 & -0.0512 & 0.0426 \\ 0.0491 & 0.9977 & 0.0477 \\ -0.0450 & -0.0455 & 0.9980 \end{bmatrix}$ $T=[-24.49\ 32.77\ 97.98]$ RMS=1.04

Figure 10. Examples of incorrectly recognized model-test pairs.

References

[1] P. Besl and N. D. Mckay. A method of registration of 3-D shapes. *IEEE Trans. Pattern Analysis and Machine Intelligence*, 14(2):239–256, 1992.

[2] B. Bhanu and H. Chen. Human ear recognition in 3D. *Workshop on Multimodal User Authentication*, pages 91–98, 2003.

[3] A. Bronstein, M. Bronstein, and R. Kimmel. Expression-invariant 3D face recognition. *Audio and Video based Biometric Person Authentication*, pages 62–70, 2003.

[4] M. Burge and W. Burger. Ear biometrics in computer vision. *Proc. Int. Conf. on Pattern Recognition*, 2:822–826, 2000.

[5] K. C. Chang, K. W. Bowyer, and P. J. Flynn. Multi-modal 2D and 3D biometrics for face recognition. *IEEE Int. Workshop on Analysis and Modeling of Faces and Gestures*, pages 187–194, 2003.

[6] K. C. Chang, K. W. Bowyer, S. Sarkar, and B. Victor. Comparison and combination of ear and face images in appearance-based biometrics. *IEEE Trans. Pattern Analysis and Machine Intelligence*, 25(9):1160–1165, 2003.

[7] C. S. Chua, F. Han, and Y. Ho. 3D human face recognition using point signatures. *Int. Conf. on Automatic Face and Gesture Recognition*, pages 233–238, 2000.

[8] D. Hurley, M. Nixon, and J. Carter. Automatic ear recognition by force field transformations. *IEE Colloquium on Visual Biometrics*, pages 7/1 –7/5, 2000.

[9] A. Iannarelli. *Ear Identification*. Forensic Identification Series. Paramont Publishing Company, 1989.

[10] A. Jain. *BIOMETRICS: Personal Identification in Network Society*. Kluwer Academic, 1999.

[11] J. C. Lee and E. Milios. Matching range images of human faces. *Proc. Int. Conf. on Computer Vision*, pages 722–726, 1990.

[12] X. Lu, D. Colbry, and A. K. Jain. Three-dimensional model based face recognition. *Proc. Int. Conf. on Pattern Recognition*, 1:362–266, 2004.

[13] G. Turk and M. Levoy. Zippered polygon meshes from range images. *Proceedings of Conf. on Computer Graphics and Interactive Techniques*, pages 311–318, 1994.

[14] P. Yan and K. B. Bowyer. 2D and 3D ear recognition. *Biometric Consortium Conference*, 2004.

[15] N. Yokoya and M. D. Levine. Range image segmentation based on differential geometry: A hybrid approach. *IEEE Trans. Pattern Analysis and Machine Intelligence*, 11(6):643–649, 1989.